

THE LUNAR MAGMA OCEAN: RECONCILING THE SOLIDIFICATION PROCESS WITH LUNAR PETROLOGY AND GEOCHRONOLOGY L.T. Elkins-Tanton¹, S. Burgess¹, Q.-Z. Yin², ¹MIT, Cambridge, MA 02139, ltelkins@mit.edu; ²Univ. California Davis, CA 95616.

Introduction: Samples of the lunar highlands led to the hypothesis that the primordial Moon was partially molten and that anorthite plagioclase was buoyantly segregated from this melt to form a crust (e.g. (1-7)). The lunar anorthosite ages span a large range of time (e.g., Fig. 1). This age span has been proposed to represent the time of solidification of the lunar magma ocean, though the ages can only be said with confidence to represent the times that the dated minerals cooled beneath their closure temperatures, and cooling can be decoupled from solidification.

Solidification of the Moon is directly dependent upon heat transfer from the interior to space. Upon formation of a conductive plagioclase lid, the heat loss regime changes from black-body radiation to conduction. The conductive lid is therefore the rate-limiting step in heat loss from the Moon, resulting paradoxically in far longer solidification times than those for larger planets without conductive lids (8).

The first goal of this study is to construct a self-consistent model for the physics and chemistry of

fractional solidification of a lunar magma ocean, with predictions for the composition and structure of the resulting lunar mantle after cumulate overturn to gravitational stability. We build on previous work (4, 9, 10). The advances of this study include tracking liquid and solid oxide components, calculation of assemblage densities using experimental data for each mineral phase, and composition and temperature tracking during solid-state cumulate overturn. *We conclude that the lunar mantle was initially azimuthally heterogeneous over a wide radius range, which may explain the compositions of mare basalts and picritic glasses.*

The second goal is to compare the timelines from magma ocean solidification models to ages from returned lunar samples and lunar meteorites, and discuss processes that might reconcile the significant timeline disagreements (Figure 1). *Here we conclude either tidal heating or another mechanism is required to delay solidification of the magma ocean.*

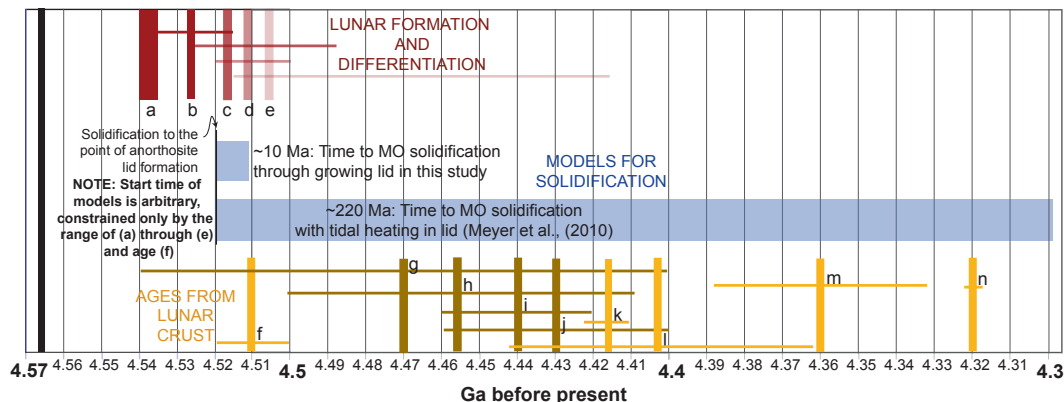


Figure 1. Ages of lunar formation and anorthositic crust formation. Black bar at left: oldest CAIs in Allende (11). In red: Moon formation and differentiation ages a: (12),

b: (13), c: (14), d: (15), e: (16). In yellow, anorthositic crust ages: f: (17), g: (18), h: (19), i: (20), j: (21), k: (22), l: (23), m: (24), n: (25). Sm-Nd ages are darker than U-Pb ages.

Methods: We consider the evolution of a convecting magma ocean of 1000 km depth using a lunar bulk silicate composition modified from (26). The model fractionally crystallizes the magma ocean and individually tracks major and trace elements; for details see (8, 27). Mantle mineral assemblages are similar to (9) and other models.

During cooling, heat is first advected in a vigorously convecting body to a free liquid surface. Unlike Solomon and Longhi (4) we propose that the Moon will not have a solid conductive lid until plagioclase flotation creates the anorthositic crust (28). Once

plagioclase begins to form a lid, cooling is calculated by solving the transient heat conduction equation in a spherical geometry for the solid lid. The lid thickness is increased during each step by the volume of plagioclase solidified during that step, assuming only plagioclase floats, thus progressively slowing the process of cooling.

Mantle overturn: Production of basalt source regions and Mg suite melting. Once solidification is complete, the modeled lunar interior invariably has an unstable density gradient (denser near the surface than at depth) under its buoyant anorthosite lid (29-

31). This unstable density gradient is created in three ways: by temperature, fractionation of magnesium and iron, and late solidification of dense iron, chromium, and titanium-bearing oxides (31, 32). A gravitationally unstable stratigraphy will overturn via Rayleigh-Taylor instabilities to a stable profile with intrinsically densest materials at the bottom (27, 32).

Both phase assemblage and composition affect density. These create an initial density profile in which some mid-level cumulates have the same density as lower-mantle cumulates, though their compositions differ. As they sink or rise under the influence of gravity, they will reach a unique depth of mutual neutral buoyancy and will stall adjacent to each other. This phenomenon serves to juxtapose magma ocean materials with different temperatures and compositions at the same depth (Figure 2).

An enduring problem in understanding the provenance of lunar basalts and volcanic glasses has been that magmas with compositions that require different melting source regions appear to have originated at similar depths in the lunar mantle (33). An azimuthally-heterogeneous lunar cumulate mantle may help explain the origin of such compositionally diverse magmas from the same range of lunar depths

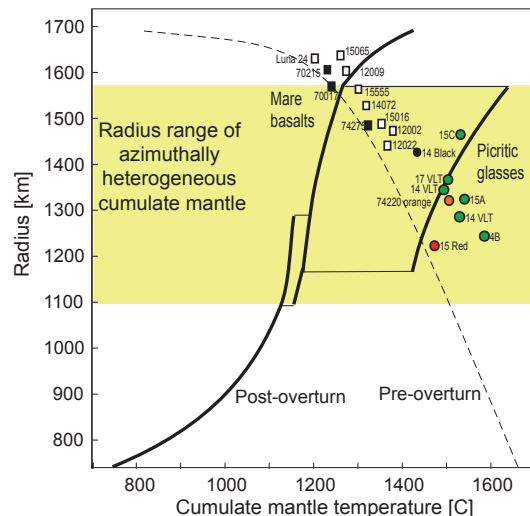


Fig. 2. Cumulate mantle temperature profiles before and after solid-state overturn. Horizontal guidelines indicate lateral compositional heterogeneity. Ref. for pressures and temperatures of origin of mare basalts (rectangles) and picritic glasses (ovals) in (34). Black and orange symbols = high Ti; green and white symbols = low Ti.

Some of the rising material may melt adiabatically. Specifically, pyroxene-bearing mid-mantle cumulates will partially melt on their ascent to the region just under the anorthositic crust. We hypothe-

size that this overturn melting may be a source for lunar Mg suite rocks and other igneous intrusives in the anorthosite flotation crust.

Time to solidification and crustal ages. Solidification of the first 80 vol% of the magma ocean, to the point that plagioclase begins to float, requires only on the order of 1,000 years. As soon as a conductive lid is established on the body solidification slows greatly, and the remaining 20 vol% of the magma ocean requires about 10 million years to solidify in this reference model (Figure 1). This solidification timeline is too short to reconcile the majority of anorthosite ages; an additional ~180 million years of delayed solidification and anorthosite crystallization and cooling is required beyond the point of complete solidification modeled here.

The likeliest process to account for the difference in time between modeled solidification and geochronology is tidal heating. Meyer et al. (10) demonstrated that tidal heating from the Earth is sufficient to slow magma ocean solidification, to hold some crustal minerals above their closure temperatures, and to melt and re-erupt portions of the crust. Cooling of crustal minerals beneath their closure temperatures may therefore have occurred at any point along this timeline and is largely decoupled from magma ocean solidification. The collective age range, from all isotope systems used, thus represents the time over which the anorthositic crust was either solidifying or resetting through tidal heat. These processes continue for ~200 Ma according to the dynamical simulations, adequate to explain the range of ages measured in lunar crustal rocks.

References: [1] Wood, *Proc. Apollo 11 Lunar Sci. Conf.*, **965** (1970). [2] Smith, *Proc. Apollo 11 Lunar Sci. Conf.*, **897** (1970). [3] Taylor, *LSC* **5**, 1287 (1974). [4] Solomon, *LPSC* **8**, 583 (1977). [5] Walker, *Geology* **5**, 425 (1977). [6.] Kaula, *JGR* **84**, 999 (1979). [7] Warren, *Ann.Rev.EPS* **13**, 201 (1985). [8] Elkins-Tanton, *EPSL* **271**, 181 (2008). [9] Snyder, *GCA* **56**, 3809 (1992). [10] Meyer, *Icarus* **208**, 1 (2010). [11] Connelly, *Chem. Geo.*, **259**, 143 (2008). [12] Yin, *Nature* **418**, 949 (2002). [13.] Kleine, *GCA* **69**, 5805 (2005). [14] Lee, *Science* **278**, 1098 (1997). [15] Lee, *EPSL* **198**, 267 (2002). [16] Touboul, *Nature* **450**, 1206 (2007). [17] Hanan, *EPSL* **84**, 15 (1987). [18] Nyquist, *LPSC*, **41** 1383 (2010). [19] Norman, *MAPS* **38**, 645 (2003). [20] Carlson, *EPSL* **90**, 119 (1988). [21] Nyquist, *GCA* **70**, 5990 (2006). [22] Nemchin, *Nature Geosci* **2**, 133 (2009). [23] Nemchin, *GCA* **70**, 1864 (2006) [24] Leont'eva, *Petrology* **13**, 193 (2005). [25] Meyer, *MAPS* **31**, 370 (1996). [26] Longhi, *GCA* **56**, 2375 (1992). [27] Elkins-Tanton, *MAPS* **38**, 1753 (2003). [28] Walker, *JGR* **90**, C585 (1985). [29] Ringwood, *LPSC* **7**, 1697 (1976). [30] Spera, *GCA* **56**, 2253 (1992). [31] Hess, *EPSL* **134**, 501 (1995). [32]. Solomatov, in *Origin of the Earth and Moon*, (2000). [33] Nyquist, *LPSC* **8**, 1383 (1977). [34] Elkins-Tanton, *EPSL* **222**, 17 (2004).